Biology Direct

RESEARCH Open Access

DEPTOR attenuates asthma progression by suppressing endoplasmic reticulum stress through SOD1

Hao Wang[1], Lei Zhang[2] and Yunxiao Shang[1*]

Abstract

Endoplasmic reticulum (ER) stress has been shown to play a pivotal role in the pathogenesis of asthma. DEPTOR (DEP Domain Containing MTOR Interacting Protein) is an endogenous mTOR inhibitor that participates in various physiological processes such as cell growth, apoptosis, autophagy, and ER homeostasis. However, the role of DEPTOR in the pathogenesis of asthma is still unknown. In this study, an ovalbumin (OVA)-induced mice model and IL-13 induced 16HBE cells were used to evaluate the effect of DEPTOR on asthma. A decreased DEPTOR expression was shown in the lung tissues of OVA-mice and IL-13 induced 16HBE cells. Upregulation of DEPTOR attenuated airway goblet cell hyperplasia, inhibited mucus hypersecretion, decreased the expression of mucin MUC5AC, and suppressed the level of inflammatory factors IL-4 and IL-5, which were all induced by OVA treatment. The increased protein expression of ER stress markers GRP78, CHOP, unfolded protein response (UPR) related proteins, and apoptosis markers in OVA mice were also inhibited by DEPTOR overexpression. In IL-13 induced 16HBE cells, overexpression of DEPTOR decreased IL-4, IL-5, and MUC5AC levels, preventing ER stress response and UPR process. Furthermore, from the proteomics results, we identified that SOD1 (Cu/Zn Superoxide Dismutase 1) may be the downstream factor of DEPTOR. Similar to DEPTOR, upregulation of SOD1 alleviated asthma progression. Rescue experiments showed that SOD1 inhibition abrogates the remission effect of DEPTOR on ER stress in vitro. In conclusion, these data suggested that DEPTOR attenuates asthma progression by suppressing endoplasmic reticulum stress through SOD1.

Keywords DEPTOR, SOD1, Asthma, ER stress, Inflammation, Apoptosis

Introduction

Asthma is one of the most common respiratory diseases affecting children and adults worldwide [1], which is characterized by variable airflow obstruction, causing dyspnea and wheezing [2]. Because of the recurrent symptoms of reversible airflow obstruction, airway hyper-responsiveness, and airway inflammation, asthma has attracted much attention from researchers [3–5]. Besides that, mucus hypersecretion caused by airway goblet cell proliferation is also one of the important clinical features of asthma. Although there has been an iterative update in the treatment of asthma, severe,

*Correspondence:
Yunxiao Shang
shangyx52111@163.com
[1]Department of Pediatric Respiratory Medicine, Shengjing Hospital of China Medical University, No. 36 Sanhao Street, Shenyang 110004, China
[2]Department of General Surgery, The Affiliated Hospital of Liaoning University of Traditional Chinese Medicine, Shenyang 110000, China

uncontrolled asthma still accounts for 5 to 10% of all patients [6, 7]. Therefore, further investigation is critical for identifying the potential targets and mechanisms for asthma.

The endoplasmic reticulum (ER) is an important organelle that plays a major role in the synthesis, folding, and structural maturation of proteins [8]. However, some genetic or environmental insults could prevent the proper folding and post-translational modification of cells in the ER, and this accumulation of misfolded proteins leads to ER stress, resulting in activation of the unfolded protein response (UPR) that aims to restore protein homeostasis [8, 9]. However, the UPR does not always overcome ER stress and restore ER functional balance. Under persistent and severe ER stress, the UPR, in turn, aggravates cellular inflammation and induces apoptosis [10, 11]. In asthma, ER stress markers, including C/EBP homologous protein (CHOP), glucose-regulated protein, and 78 kDa (GRP78), are increased [12, 13]. However, 4-PBA, a chemical chaperone that inhibits ER stress/UPR, ameliorates the pathologic features of OVA mice [12]. Although studies have confirmed that ER stress and UPR activation are critical for the induction and maintenance of asthma [12, 14, 15], the complex regulatory mechanisms remain to be elucidated.

DEP Domain Containing MTOR Interacting Protein (DEPTOR), an endogenous mTOR inhibitor, is the focus of research on the occurrence and development of human malignancies [16, 17]. DEPTOR is involved in a variety of physiological processes, such as cell growth, apoptosis, autophagy, and endoplasmic reticulum homeostasis, by inhibiting mTOR kinase activity [16, 18, 19]. In alcoholic liver disease, overexpression of DEPTOR suppressed mTORC1 signaling and ameliorated inflammation and acute-on-chronic liver injury [20]. Recent reports have also confirmed that DEPTOR inhibits ER stress and apoptosis in chondrocytes by directly regulating downstream protein activity, thereby alleviating the progression of osteoarthritis [21], and its function is independent of mTOR signaling. Furthermore, the upregulation of DEPTOR inhibits the production of inflammatory factors and activation of the NF-κB pathway in nasal mucosal cells from patients with rhinitis [22]. However, the roles and mechanisms of DEPTOR in the regulation of the physiological and pathological asthma processes in vivo are unknown.

Therefore, in the present study, we used an OVA-induced asthma mouse in vivo and IL-13-treated 16HBE cells in vitro to investigate the role and potential regulatory mechanism of DEPTOR in asthma progression. Our results demonstrated that DEPTOR is suppressed in OVA mice. Upregulation of DEPTOR could protect mice from asthma-induced injury, and this protective effect may be associated with the downstream factor SOD1 (Cu/Zn Superoxide Dismutase 1).

Materials and methods

Data collection and analysis

To explore the expression of DEPTOR in OVA mice, Gene Expression Omnibus (GEO) databases GSE6858, GSE49694, GSE49705, and GSE13382 were used. Data were analyzed by GEO2R (https://www.ncbi.nlm.nih.gov/geo/geo2r/).

Mice asthma model

Eight-week-old female BALB/c mice were randomly divided into four groups (Control, OVA, OVA+Vector^{AAV2}, OVA+DEPTOR^{AAV2}) and adaptively fed for one week (12 h light and 12 h dark, temperature 22±1℃, humidity 45–55%) with free to eat and drink. Mice were sensitized by intraperitoneal (i.p.) injection of 20 μg of OVA (A800616, Macklin, China) emulsified in 2.25 mg of aluminum hydroxide in a total volume of 100 μl on days 0 and 10. Upregulation of DEPTOR in mice was achieved by adeno-associated virus 2 (AAV2) infection. On day 14, Vector^{AAV2} or DEPTOR^{AAV2} at a dose of 5×10^{10} plaque-forming units in 20 μl of PBS per mouse was administered to mice through intratracheal injection. We challenged animals via airways with a nebulized 1% OVA on days 28, 29, and 30, for 30 min a day. A control group of mice received saline solution i.p. and were challenged with 1% OVA. After 48 h (day 32), mice were sacrificed and serum, BALF, and lung tissues were collected for further use.

BALF collection and analysis

After the mice were anesthetized, the trachea was exposed through a median neck opening. A small incision was made close to the head and a 1 ml syringe was inserted into the trachea. A slow bolus of 500 μL of precooled PBS was administered and the mouse chest was gently rubbed for 15 to 20 s, after which lavage fluid was aspirated. This step was repeated three times. After centrifugation, total inflammatory cells were counted by trypan blue exclusion using a hemacytometer, and the total number of cells per milliliter of BALF was calculated based on the dilution and the volume of the cell counter plate. Similar to reported studies [23, 24], macrophages, eosinophils, neutrophils, and lymphocytes in BALF were stained and counted with a Diff-Quick staining kit (G1541, Solarbio, China) according to the manufacturer's instructions. Briefly, BALF was prepared as the cell slides. After drying, the slides were fixed with methanol for 20 s. Then, Diff-Quik I staining was performed for 5–10 s followed by Diff-Quik II staining for 10–20 s. After that, the cells were observed under a microscope. Different types of cells were distinguished according to cell size

and morphology after staining. The proportion of macrophages, eosinophils, neutrophils, and lymphocytes in 200 inflammatory cells was calculated. Then, the number of each inflammatory cell in each milliliter of BALF was calculated.

Detection kits

OVA-specific IgE in mouse serum was tested with the Mouse OVA specific-IgE ELISA Kit (EM1254, Fntest, China). The level of inflammatory factors IL-4 and IL-5 were measured with the ELISA kits (EK205, EK204, EK105, and EK104) that were obtained from Liankebio (China). Protein concentration was measured by BCA kit (P0011, Beyotime, China). Optical density values were read using a microplate reader (ELX-800, BIOTEK, US).

Real-time quantitative PCR (q-PCR)

Total RNA of cells or lung tissues from mice was extracted using TRIpure reagent (RP1001, BioTeke, China), and the concentration was detected by UV spectrophotometer (NANO 2000, Thermo Fisher Scientific, USA). The obtained RNA was reversed to complementary DNA with RNase inhibitor (BL780A, Biosharp, China) and BeyoRT II M-MLV reverse transcriptase (D7160L, Beyotime, China). q-PCR was performed by using 2×Taq PCR Master Mix (PC1150, Solarbio, China) and SYBR Green (SY1020, Solarbio, China) with PCR instrument (Exicycler 96, Bioneer, Korea). Relative mRNA levels of target genes were calculated by the $2^{-\triangle\triangle CT}$ assay.

Primer information: homo SOD1 forward: 5'-GGTCC TCACTTTAATCCTCT-3', reverse: 5'-CTTCATTTCCA CCTTTGC; homo DEPTOR forward: 5'-GCCACCACG AGGAAAGA-3', reverse: 5'-CCTCAGGCAGAAGGGA C-3'; mus MUC5AC forward: 5'-CGTGGTCTGGAAGG ATGCTAT-3', reverse: 5'-GAACTGTTGCCCGTTGTAG GT-3'; mus DEPTOR forward: 5'-GACGGCACCATCTC AAA-3', reverse: 5'-GTCCCATCATCCTTCCTAA-3'.

Western blotting

Total protein was extracted from tissues or cells by RIPA lysate (PR20001, Proteintech, China) with the addition of 1% protease inhibitors/phosphatase inhibitors (PR20032, PR20015, Proteintech, China). Concentration was determined by the BCA kit (PK10026, Proteintech, China). Protein was separated by SDS-PAGE (PR20004, Proteintech, China) and transferred to a PVDF membrane (LC2005, Thermo Fisher Scientific, USA). After blocking of non-specific binding with blocking buffer (PR20011, Proteintech, China) for 5 min, the membranes were treated with primary antibodies at 4℃ overnight followed by treatment with secondary antibody for 40 min at room temperature (RT). Protein bands were visualized using the enhanced chemiluminescence reagents (PK10003, Proteintech, China).

Antibody information

DEPTOR antibody (1:5,000, Proteintech Cat# 20985-1-AP, RRID: AB_11182391), p-PERK^{Thr982} antibody (1:1,000, Beyotime Cat# AF5902, China), PERK antibody (1:1,000, ABclonal Cat# A18196, RRID: AB_2861973), p-eIF2α^{S51} antibody (1:1,000, ABclonal Cat# AP0692, RRID: AB_2863809), eIF2α antibody (1:1,000, ABclonal Cat# A21221), p-IRE1α^{Ser724} antibody (1:1,000, Abcam Cat# ab48187, RRID: AB_873899), IRE1α antibody (1:1,000, ABclonal Cat# A21021), SOD1 antibody (1:500, ABclonal Cat# A12537, RRID: AB_2861671), CHOP antibody (1:3,000, ABclonal Cat# A0221, RRID: AB_2757035), cleaved-caspase-3 antibody (1:1,000, Affinity Biosciences Cat# AF7022, RRID: AB_2835326), cleaved-PARP antibody (1:1,000, Affinity Biosciences Cat# AF7023, RRID: AB_2835327), ATF6 antibody (1:500, ABclonal Cat# A0202, RRID: AB_2757016) (ABclonal A0202), goat anti-rabbit IgG-HRP (1:10,000, Proteintech Cat# SA00001-2, RRID: AB_2722564).

Cell treatment

The 16HBE cells were cultured in RPMI-1640 (31800, Solarbio, China) supplemented with 10% fetal bovine serum (11011−8611, Tiangangbio, China) in an incubator with 5% CO_2 at 37℃. DEPTOR overexpression or SOD1 knockdown in cells was accomplished by transfecting DEPTOR overexpression plasmid or SOD1 siRNA into 16HBE cells with the help of lipofectamine 3000 (L3000015, Invitrogen, USA). After transfection, 10 ng/ml IL-13 (RP01320, ABclonal, China) was used to treat cells. In some sections, cells were treated with ER-Tracker Red (MX4353, Maokangbio, China), and the images were taken by a microscope (OLYMPUS, Japan).

Immunohistochemical (IHC) staining

Lung tissues isolated from different experimental mice were paraffin-embedded and then sliced into 5 μm-thick sections. Before staining, the sections were deparaffinized with xylene and gradually immersed in different concentrations of ethanol. After antigen retrieval, the sections were incubated with 3% H_2O_2 for 15 min to eliminate the activity of endogenous peroxidase and then blocked with 1% BSA (A602440-0050, Sangonbio, China) for 15 min. Then, sections were incubated with DEPTOR (Proteintech Cat# 20985-1-AP, RRID: AB_11182391), SOD1 (ABclonal Cat#A22594), or MUC5AC (Abcam Cat# ab198294, RRID: AB_2894855) antibody (1:200) overnight at 4℃, followed by goat anti-rabbit IgG/HRP (1:100, Solarbio Cat# SE134, RRID: AB_2797593) for 45 min at RT. After that, sections were added with DAB solution (C520017, Sangonbio, China) and counterstained with hematoxylin (H8070, Solarbio, China) for 3 min. Sections were gradually immersed in different concentrations (75%, 85%, 95%) of ethanol and xylene.

Images were taken with a microscope (OLYMPUS, Japan). The rate of DEPTOR or SOD1 positive cells was calculated.

Histology staining

For periodic acid-Schiff (PAS) staining, tissue sections were stained in periodic acid for 10 min and Schiff's Reagent (DG0005, Leagene, China) for 15 min, respectively. After counterstaining with hematoxylin for 2 min, sections were rinsed with water and immersed in ethanol and xylene. PAS-positive cells were displayed as the percentage. For hematoxylin and eosin (H&E) staining, tissue sections were stained in hematoxylin (H8070, Solarbio, China) for 5 min, 1% hydrochloric acid in alcohol for 3 s, and eosin solution (A600190, Sangonbio, China) for 3 min, respectively. Then, sections were immersed in ethanol and xylene. Stained sections were photographed and analyzed under a microscope (OLYMPUS, Japan).

Immunofluorescence (IF) staining

Cells were fixed using 4% paraformaldehyde for 15 min. Following permeabilization with 0.1% Triton X-100 (ST795, Beyotime, China) for 30 min and blocking with 1% BSA (A602440-0050, Sangonbio, China) for 15 min, MUC5AC antibody (1:200, Abcam Cat# ab198294, RRID: AB_2894855) was added to the sections overnight at 4℃. The sections were then treated using a goat anti-rabbit IgG, Cy3 conjugate (1:200, Proteintech Cat# SA00009-2, RRID: AB_2890957) for 60 min at RT, and cell nucleus was stained by DAPI (D106471-5 mg, Aladdin, China). Images were taken with a microscope (OLYMPUS, Japan).

Lung tissues from mice were paraffin-embedded and then sliced into 5 μm-thick sections. Before staining, the sections were deparaffinized with xylene and gradually immersed in different concentrations of ethanol. After antigen retrieval, the sections were blocked with 1% BSA for 15 min. The other steps were the same as the cell samples. Antibody information: GRP78 (1:200, Proteintech Cat# 11587-1-AP, RRID: AB_2119855), CHOP (1:200, ABclonal Cat# A0221, RRID: AB_2757035), and goat anti-rabbit IgG, Cy3 conjugate (1:200, Proteintech Cat# SA00009-2, RRID: AB_2890957).

TUNEL staining

Cell death in lung tissues was tested by the In Situ Cell Death Detection Kit (12156792910, Roche, Switzerland). Before staining, the Sect. (5 μm) were deparaffinized with xylene and gradually immersed in different concentrations of ethanol. Sections were permeabilized with 0.1% Triton X-100 (ST795, Beyotime, China). Then, 50 μl of TUNEL solution was added, and the sections were incubated at 37℃ for 60 min in the dark. After rinsing with PBS, sections were counterstained with DAPI (D106471-5 mg, Aladdin, China) for 5 min in the dark. Fluorescent images were obtained using a fluorescent microscope (OLYMPUS, Japan).

Cell apoptosis

Cell death in 16HBE cells was tested by Annexin V-FITC/PI double staining apoptosis detection kit (KGA106, Keygenbio, China). After centrifugation, cells were resuspended in 500 μl binding buffer. After mixing with 5 μl AnnexinV-FITC, 5 μl propidium iodide was added. Cells were then incubated at RT for 15 min in the dark, and detected by flow cytometry (NovoCyte, Agilent, USA).

Proteomics and data analysis

To search for the potential downstream factors of DEPTOR, we collected DEPTOR overexpressed cells (IL-13+Vector and IL-13+DEPTOR) for label-free proteomics. LC-MS analysis was achieved on a RIGOL L-3000 system. The mobile phase A was 0.1% formic acid and 100% water, and mobile phase B was 0.1% formic acid and 80% acetonitrile. The peptides were analyzed with a Q-Exactive mass spectrometer. After analysis, we selected the differently expressed proteins by $|Log_2FC| \geq 1$ & p-value < 0.05.

Statistical analysis

Results were shown as the mean and standard deviation (SD), and $P < 0.05$ was considered statistically significant. The statistical significance of the results was determined by GraphPad Prism. The unpaired Student's t-test was utilized to compare the two groups, while a one-way analysis of variance was employed to compare multiple groups.

Results

DEPTOR is suppressed in asthma mice and inhibits mucus hypersecretion

Based on GEO databases, we found the decreased expression of DEPTOR in OVA mice (Fig. 1a). Subsequently, we used OVA to induce an allergic mouse model (Fig. 1b), and the enhanced level of OVA-specific IgE was confirmed in the serum of mice (Fig. 1c). Consistent with the database results, we also found that DEPTOR was significantly decreased in OVA mice (Fig. 1d-e). Then, we forced the expression of DEPTOR in OVA mice, and the upregulated expression was confirmed by WB (Fig. 1f) in the lung tissues of OVA mice. IHC images and quantification data also reflected that DEPTOR was highly expressed in the lung tissues of OVA mice after DEPTOR overexpression ($p < 0.05$, Fig. 1g-h). Besides that, the enhanced level of OVA-specific IgE in OVA mice was suppressed by DEPTOR overexpressing (Fig. 1i, $p < 0.01$).

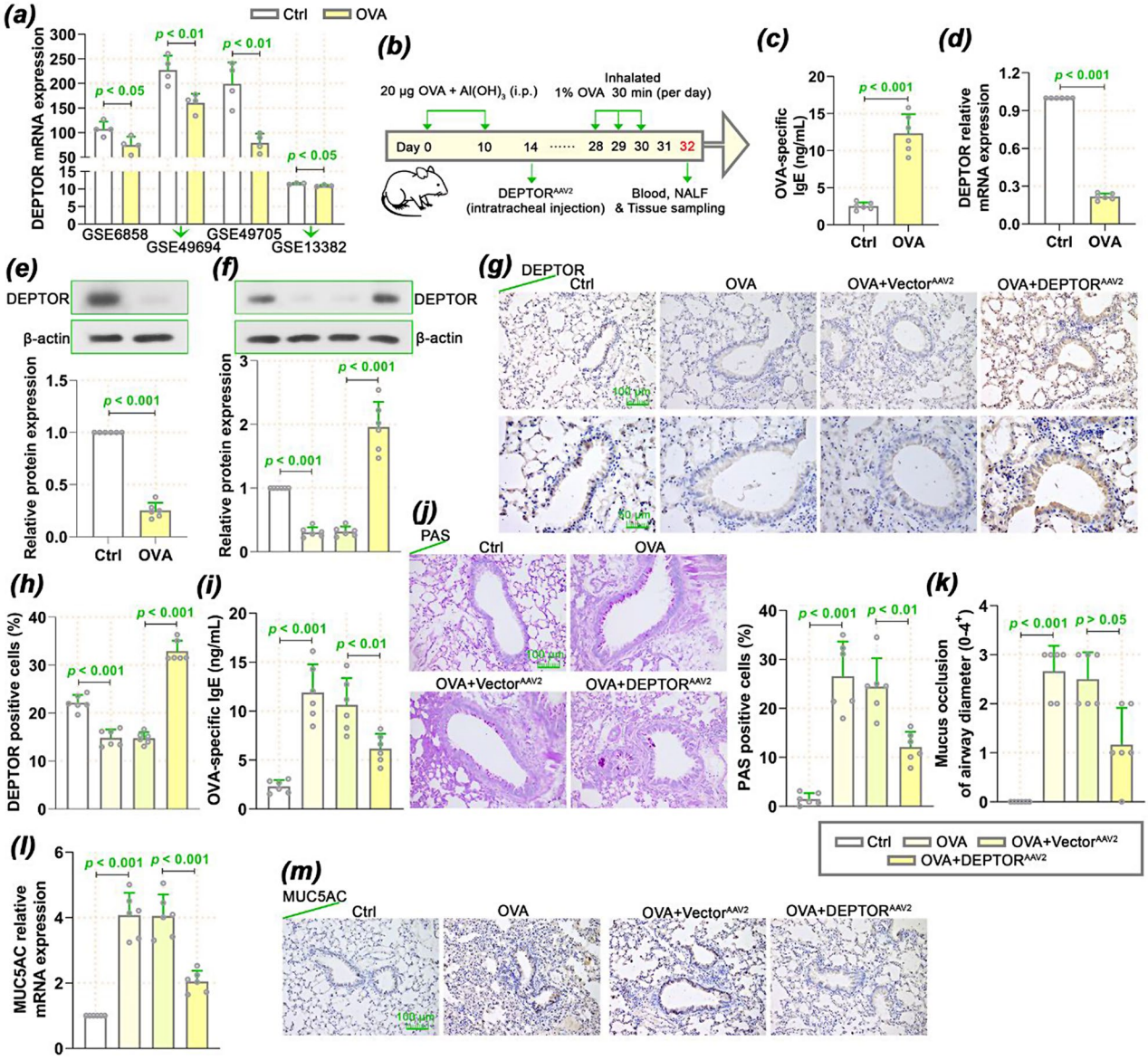

Fig. 1 DEPTOR is suppressed in asthma mice. (**a**) The mRNA expression of DEPTOR in control or OVA-treated mice from GEO databases GSE6858, GSE49694, GSE49705, and GSE13382. (**b**) Protocol for OVA allergen-induced mouse model of asthma. (**c**) Serum level of OVA-specific IgE in OVA mice. (**d**) The mRNA expression of DEPTOR in OVA mice. (**e**) The protein expression and quantification data of DEPTOR in OVA mice. (**f**) The protein expression and quantification data of DEPTOR in different groups of OVA mice. (**g-h**) The IHC images and positive cell rate of DEPTOR in the lung tissues of OVA mice. (**i**) Serum levels of OVA-specific IgE in DEPTOR upregulated OVA mice. (**j**) PAS staining images and positive cells rate in lung tissues of OVA mice. (**k**) The occlusion of airway diameter by mucus in the lung tissues was quantified based on PAS staining. (**l**) The mRNA expression of MUC5AC in lung tissues of OVA mice. (**m**) The IHC staining images of MUC5AC in lung tissues of OVA mice. Six mice per group ($N=6$). Data were expressed as mean ± SD

Then, we measured the effect of DEPTOR on airway mucus production in OVA mice. PAS staining images showed that OVA-induced goblet cell hyperplasia and mucus production could be rescued by DEPTOR overexpression (Fig. 1j). Overexpression of DEPTOR reduced the rate of PAS-positive cells ($p<0.05$, Fig. 1j) and the score of mucus obstructed airway diameter (Fig. 1k, $p=0.051$) in lung tissues of OVA mice. Similarly, the mRNA (Fig. 1l) and protein (Fig. 1m) expression of mucin MUC5AC in lung tissues were lower in DEPTOR-overexpressed OVA mice than that of vector-infected OVA mice.

DEPTOR restrains the inflammation in asthmatic mice

Then, we evaluated the effect of DEPTOR on inflammation of OVA mice. H&E staining images (Fig. 2a) and inflammation scores (Fig. 2b) showed large amounts of inflammatory cells infiltrating the airway, with congestive edema of the bronchial mucosa in OVA-induced mice, while these trends were reversed by DEPTOR

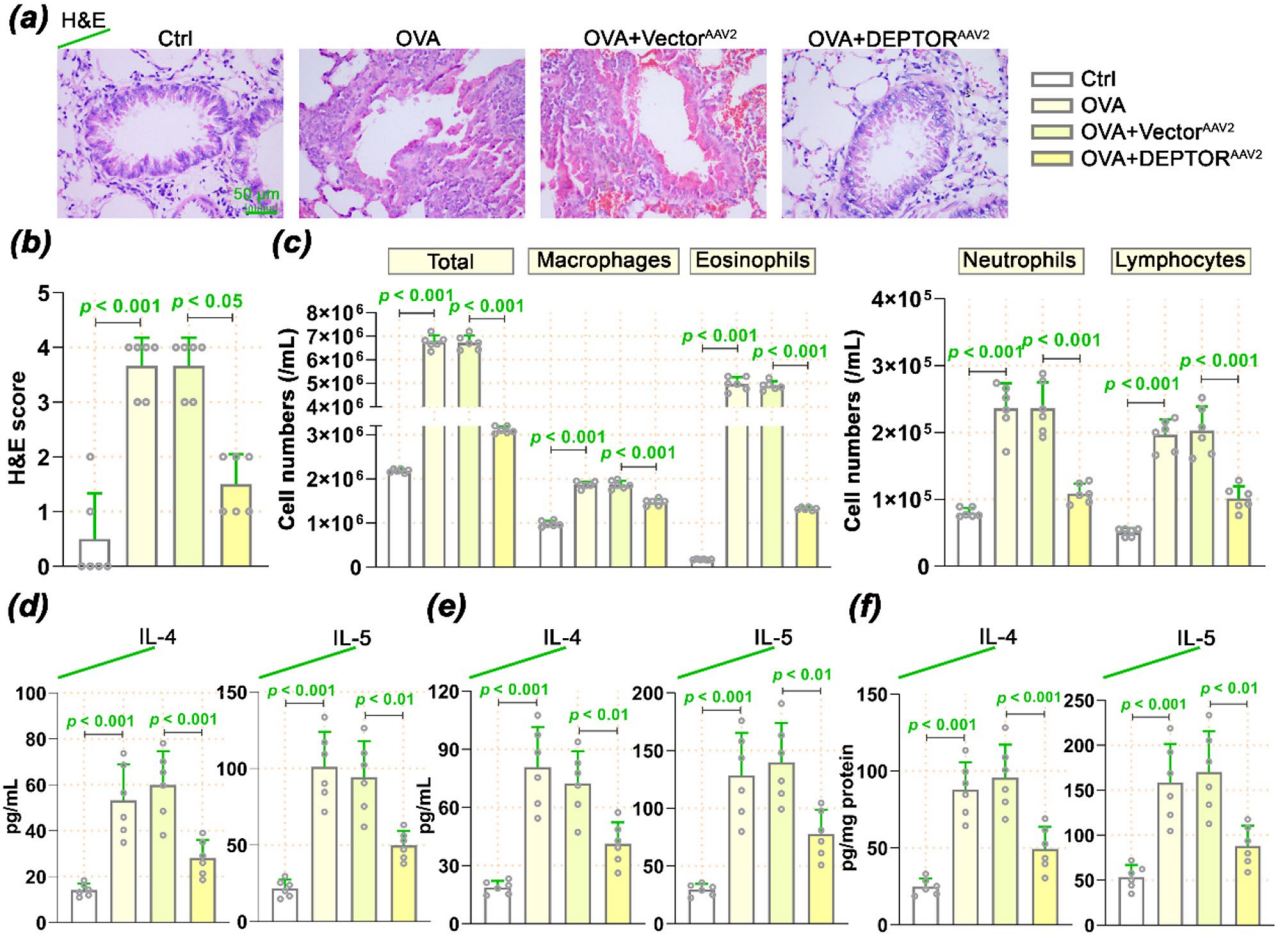

Fig. 2 Effect of DEPTOR on inflammation in asthmatic mice. (**a-b**) H&E staining images and scores of lung sections from OVA mice. (**c**) Count of cells in BALF of OVA mice. Levels of inflammatory cytokines IL-4 and IL-5 in serum (**d**), BALF (**e**), or lung tissues (**f**) of OVA mice. Six mice per group ($N=6$). Data were expressed as mean ± SD

overexpression. The inflammatory cells in BALF were also counted (Fig. 2c). Compared with the control, mice in the OVA and the vector (OVA+vector) groups displayed severe airway inflammatory responses, including extensive infiltration of inflammatory cells into the BALF. DEPTOR overexpression induced a remarkable decrease in not only the total cell counts but also the numbers of macrophages, eosinophils, neutrophils, and lymphocytes compared with vector-infected OVA mice. In addition, the upregulation of DEPTOR also reduced the levels of inflammatory factors IL-4 and IL-5 in serum (Fig. 2d), BALF (Fig. 2e), and lung tissues (Fig. 2f).

DEPTOR prevents ER stress and cell apoptosis in asthmatic mice

Previous studies have shown that ER stress and followed UPR activation are critical for the induction and maintenance of asthma. Therefore, to investigate whether the protective role of DEPTOR in OVA mice was mediated by the regulation of DEPTOR on ER stress, we measured the protein expression of key markers in this process. IF images showed that the red fluorescence of GPR78 and CHOP is enhanced, while overexpression of DEPTOR inhibited this trend, and reduced the red fluorescence in OVA mice (Fig. 3a). In mammals, the UPR comprises three signaling pathways regulated downstream of the ER membrane proteins IRE1, ATF6, and PERK [25]. In lung tissues of mice, western blot and quantification results showed that OVA promotes the phosphorylation level of $PERK^{Thr982}$, $eIF2\alpha^{S51}$, and $IRE1\alpha^{Ser724}$, and increases the expression of nuclear ATF6. In contrast, the upregulation of DEPTOR reversed these results in OVA mice (Fig. 3b-c). These results implied that DEPTOR inhibits ER stress and UPR activation in asthmatic mice. Since CHOP plays an important role in ER stress-induced apoptosis, we measured the effect of DEPTOR on apoptosis in OVA mice. As shown in Fig. 3d and e, OVA-induced apoptosis in mice lung tissues, showed an increased percentage of TUNEL-positive cells in mice lung tissues. Also, OVA increased the protein expression of CHOP, cleaved PARP, and cleaved caspase 3 in mice lung tissues ($p<0.05$, Fig. 3f-h). However, the upregulation of

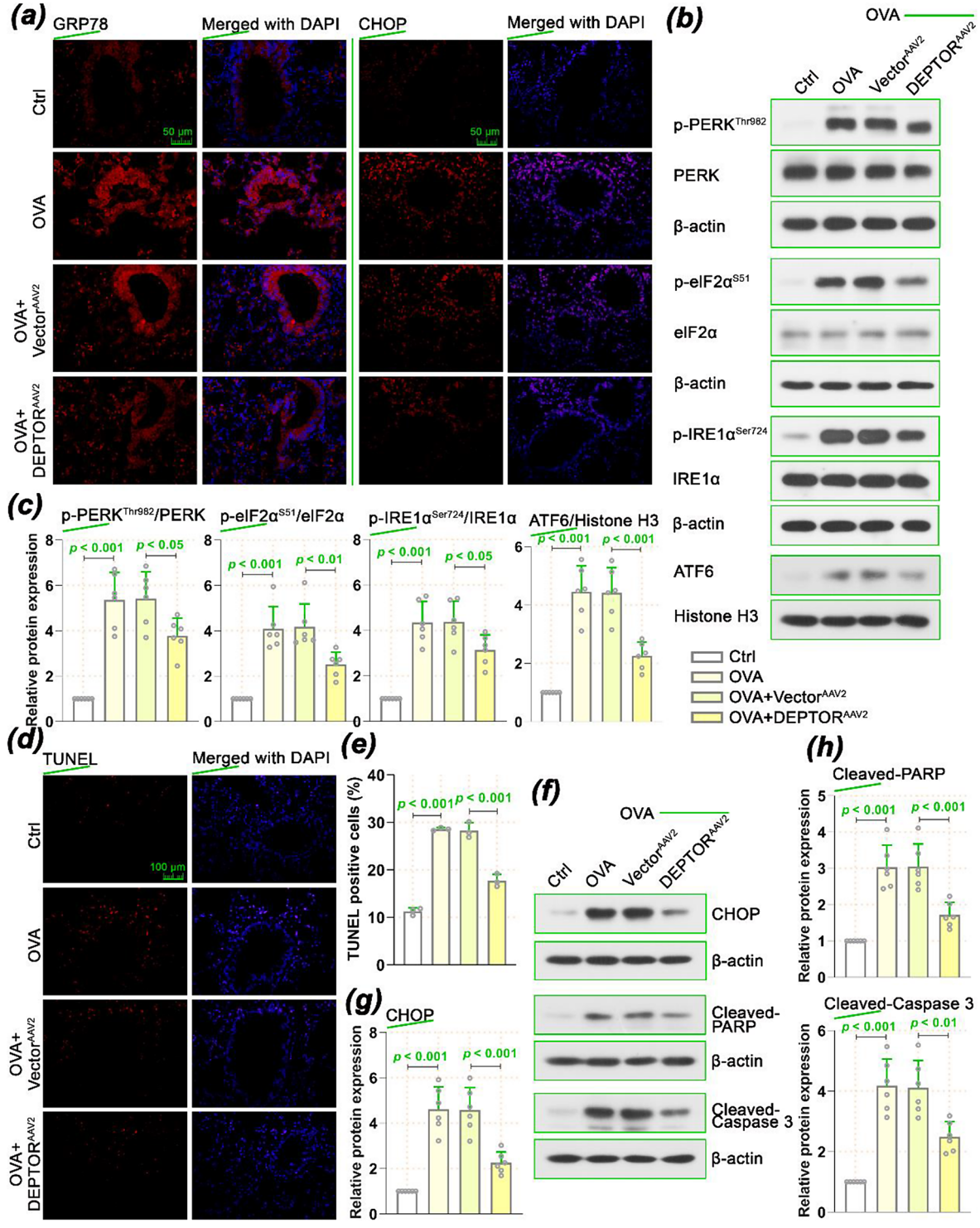

Fig. 3 Effect of DEPTOR on ER stress and apoptosis in asthmatic mice. (**a**) The expression of GRP78 or CHOP in lung tissues of OVA mice was detected by IF staining. (**b-c**) Western blot and quantification results of p-eIF2α^{S51}, p-PERK^{Thr982}, p-IRE1α^{Ser724}, and nuclear ATF6 expression in lung tissues of OVA mice. (**d-e**) TUNEL staining images and quantification results were used to detect apoptosis in lung tissues of OVA mice. (**f-h**) Protein expression of CHOP, cleaved-caspase-3, and cleaved-PARP in lung tissues of OVA mice. Six mice per group ($N=6$). Data were expressed as mean ± SD

DEPTOR reversed these trends in OVA mice, indicating that DEPTOR may alleviate apoptosis in asthmatic mice by inhibiting ER stress.

DEPTOR suppresses mucus production and inflammation in IL-13 treated 16HBE cells

Then, the bronchial epithelial cell 16HBE was administered with interleukin-13 (IL-13) to generate a cell injury model for exploration. Cells were treated with 10 ng/ml IL-13 for 24 h at 37℃. In 16HBE cells, the addition of IL-13 reduced the mRNA and protein expression of DEPTOR (Fig. 4a-b). Subsequently, we upregulated DEPTOR in 16HBE (Fig. 4c-d) and IL-13 treated 16HBE cells (Fig. 4e-f), and the mRNA and protein expression was verified by qPCR and western blot. IF images showed that the red fluorescence of MUC5AC is enhanced in IL-13 treated 16HBE cells, while overexpression of DEPTOR reduced the red fluorescence in cells (Fig. 4g). Similarly, overexpression of DEPTOR reduced the enhancement of IL-4 and IL5 in 16HBE cells, which were induced by IL-13 (Fig. 4h). These results reflected that DEPTOR relieves IL-13 induced cell injury in 16HBE.

DEPTOR inhibits ER stress and apoptosis in IL-13 treated 16HBE cells

Then, we measured the effect of DEPTOR on ER stress in IL-13 treated 16HBE cells. As shown in Fig. 5a, the red fluorescence of the ER tracker is enhanced in IL-13 treated 16HBE cells, while overexpression of DEPTOR reduced it. Western blot and quantification results showed that upregulation of DEPTOR inhibits the phosphorylation level of PERK^{Thr982}, eIF2α^{S51}, and IRE1α^{Ser724}, and suppresses the expression of nuclear ATF6 in cells, which were induced by IL-13 (Fig. 5b-c). Meanwhile, in IL-13 treated 16HBE cells, DEPTOR overexpressing alleviated cell apoptosis (Fig. 5d-e), and reduced the protein expression of CHOP, cleaved PARP, and cleaved caspase

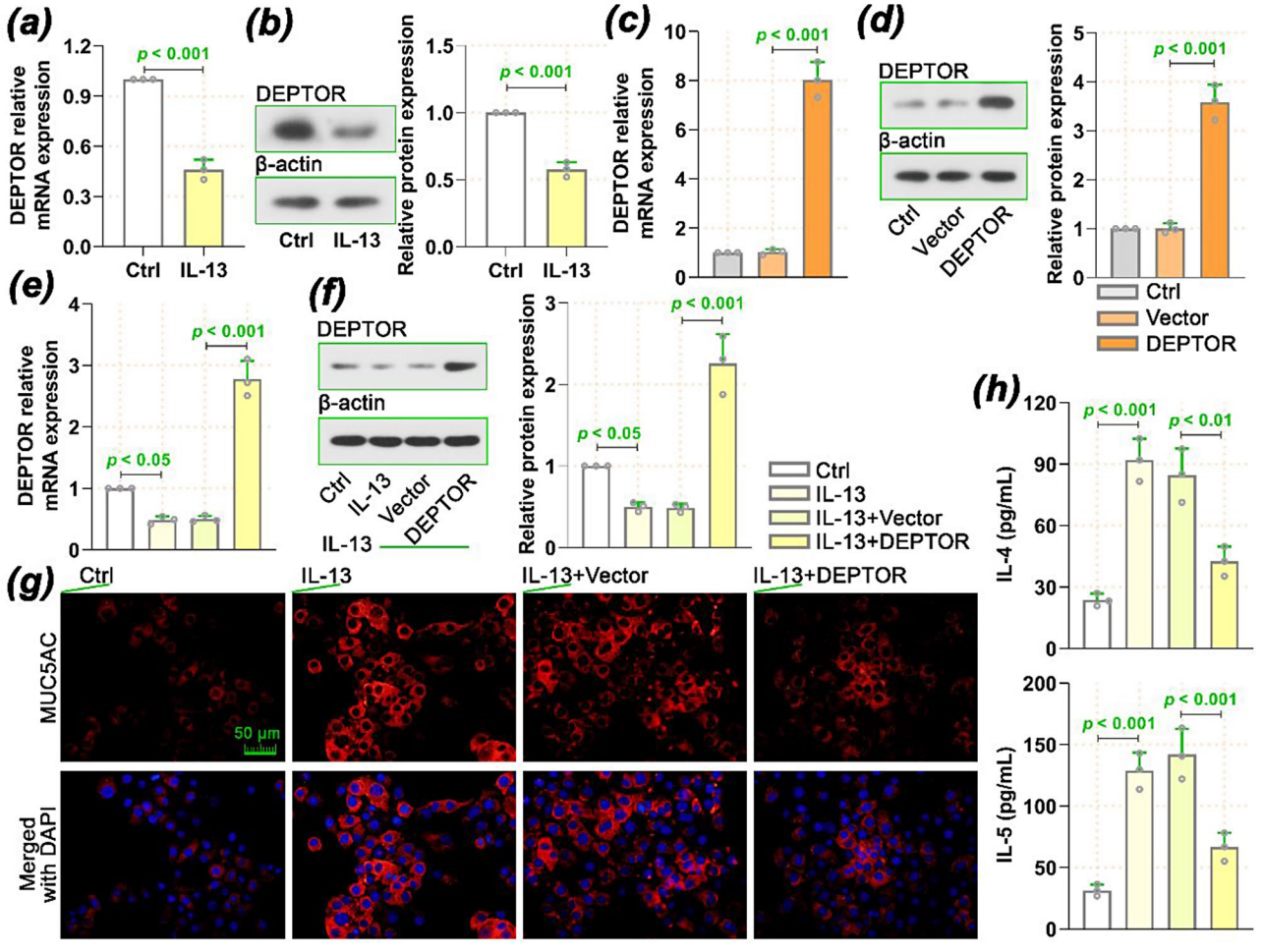

Fig. 4 Effect of DEPTOR on mucus production and inflammation in IL-13 treated 16HBE cells. Cells were treated with 10 ng/ml IL-13 for 24 h at 37℃. (**a-b**) The mRNA and protein expression of DEPTOR in IL-13 treated 16HBE cells. DEPTOR was overexpressed in 16HBE cells and the result was confirmed by qPCR and western blot (**c-d**). (**e-f**) The mRNA and protein expression of DEPTOR in IL-13 treated 16HBE cells. (**g**) IF staining images of MUC5AC in IL-13 treated 16HBE cells. (**h**) Levels of IL-4 and IL-5 in IL-13 treated 16HBE cells. Data were expressed as mean ± SD

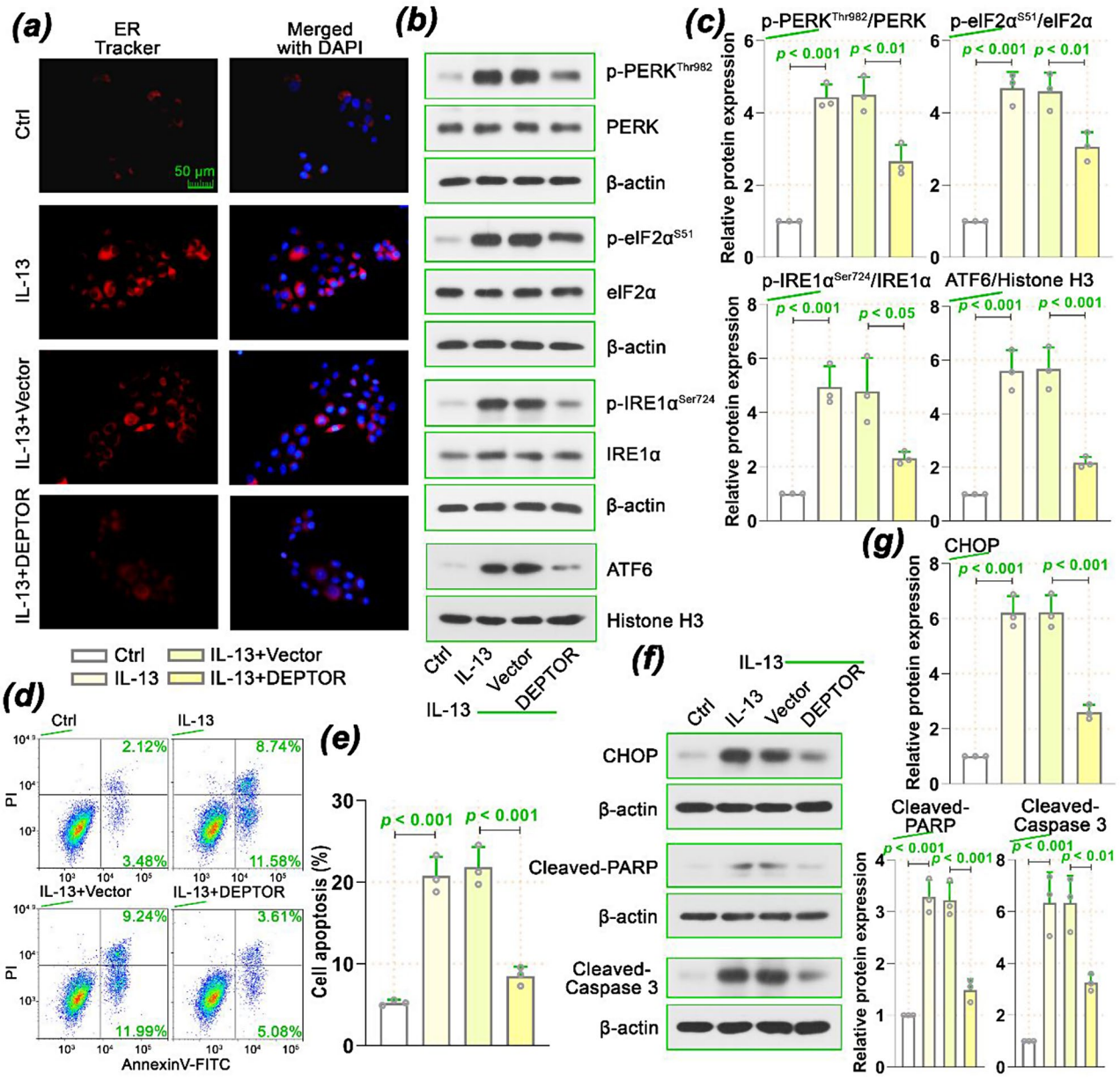

Fig. 5 Effect of DEPTOR on ER stress and followed apoptosis in IL-13 treated 16HBE cells. (**a**) IF technology traces ER in IL-13 treated 16HBE cells. (**b-c**) Western blot and quantification results of p-eIF2α^{S51}, p-PERK^{Thr982}, p-IRE1α^{Ser724}, and nuclear ATF6 expression in IL-13 treated 16HBE cells. (**d-e**) Cell apoptosis in IL-13 treated 16HBE cells was tested by flow cytometry. (**f-g**) Western blot and quantification results of CHOP, cleaved-caspase-3, and cleaved-PARP expression in IL-13 treated 16HBE cells. Data were expressed as mean ± SD

3 (Fig. 5f-g). These results reflected that DEPTOR alleviates ER stress and apoptosis in IL-13 treated 16HBE cells.

Proteomics was used to explore the possible downstream mechanism of DEPTOR

After confirming the essential role of DEPTOR in asthmatic ER stress, we performed proteomics in DEPTOR-overexpressing 16HBE cells to identify the potential downstream factors of DEPTOR. After data analysis, a total of 122 differentially expressed proteins ($|Log_2FC| \geq 1$, $p < 0.05$) were obtained. The total of 122 differentially expressed proteins was presented with volcano plot (Fig. 6a) and cluster heatmap (Fig. 6b). GO and KEGG functional enrichment analyses were also applied to these genes, and the top 10 enriched terms in GO (BP: biological process, CC: cellular component, MF: molecular function) and KEGG were displayed (Fig. 6c). Besides that, the top 10 up- and down-regulated proteins were exhibited by heatmap (Fig. 6d). Among these factors, SOD1 was noticed. SOD1 is an important antioxidant enzyme that is widely known for its ROS-scavenging activity. In DEPTOR overexpressed 16HBE cells, SOD1

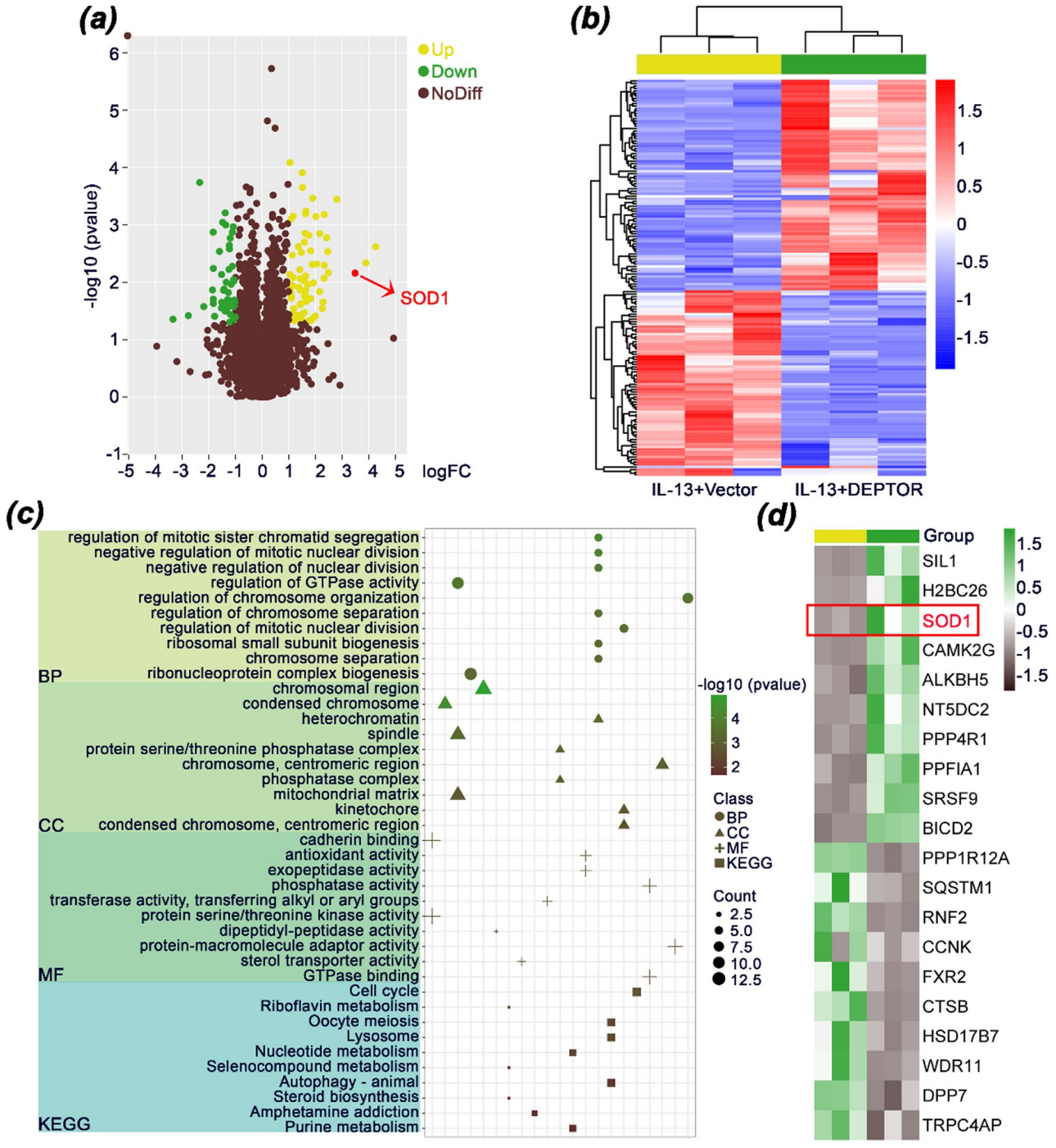

Fig. 6 Proteomics analysis in IL-13 treated 16HBE cells with DEPTOR upregulation. (**a**) Volcano plot of all up- or down-regulated differential expressed proteins in IL-13 treated 16HBE cells upon DEPTOR upregulation. (**b**) Cluster heatmap of all differentially expressed proteins. (**c**) GO and KEGG enrichment analyses of all differentially expressed proteins were analyzed by the DAVID analysis tool. (**d**) The protein expression of TOP 10 up- and down-regulated differentially expressed proteins was exhibited by heatmap

was significantly upregulated ($Log_2FC=3.5$, $p<0.01$). Study has shown that upregulation of SOD1 reduces ROS generation, inhibiting oxidative stress and attenuating ER stress-induced apoptosis in vascular endothelial cells [26]. Accordingly, we suspected that SOD1 may also participate in the beneficial role of DEPTOR in asthma progression.

SOD1 mediated the beneficial role of DEPTOR in Asthma

The expression of SOD1 in DEPTOR upregulated 16HBE cells and OVA mice was detected at first. As shown in Fig. 7a and b, upregulation of DEPTOR promoted the expression of SOD1 both in IL-13 induced 16HBE cells and OVA mice.

Then, SOD1 was upregulated in 16HBE cells to evaluate the effect on asthma progression (Fig. 7c) and verified the mRNA and protein expression of SDO1 in IL-13 treated cells (Fig. 7d-e). IF images and detection kit results showed that IL-13 induced MUC5AC protein expression (Fig. 7f) and inflammatory cytokines IL-4 and IL-5 levels (Fig. 7g), while upregulation of SOD1 reversed this trend, inhibited mucus hypersecretion and inflammation. Besides that, in IL-13-treated 16HBE cells, SOD1 upregulation decreased the promotion of IL-13 on ER stress (Fig. 7h) and cell apoptosis (Fig. 7i-j) and decreased the protein expression of CHOP, cleaved-caspase3, and cleaved-PARP (Fig. 7k).

After that, SOD1 was suppressed in 16HBE cells, and the results were verified by qPCR (Fig. 8a) and western blot (Fig. 8b). Resue experiments showed that SOD1 knockdown could reverse the protective effect of DEPTOR on MUC5AC protein expression (Fig. 8c), inflammatory cytokines IL-4 and IL-5 levels (Fig. 8d), ER stress (Fig. 8e), cell apoptosis (Fig. 8f), and related markers (Fig. 8g-h) in IL-13 induced 16HBE cells. Therefore, we implied that SOD1 mediates the beneficial role of DEPTOR in asthma-induced malignant behaviors.

Discussion

Asthma is a common chronic respiratory disease that affects people's health worldwide [27]. In this work, we uncovered the essential role of DEPTOR in asthma development. Either in OVA-induced mice or IL-13 treated 16HBE cells, DEPTOR was downregulated. Upregulation of DEPTOR attenuated airway mucus hypersecretion and inflammation. Besides that, overexpression of DEPTOR suppressed ER stress and UPR activation, and decreased cell apoptosis. Furthermore, SOD1 mediated the beneficial role of DEPTOR in asthma, and SOD1 inhibition abrogated the remission effect of DEPTOR on ER stress.

From previously reported studies, we found that DEPTOR plays a protective role in alcoholic liver disease [20], osteoarthritis [21], and rhinitis [22]. However, its role in asthma remains unclear. GEO databases GSE6858, GSE49694, GSE49705, and GSE13382 displayed a decreased mRNA expression of DEPTOR in OVA mice. Similarly, we also confirmed the decreased level of DEPTOR in the lung tissues of OVA mice. Therefore, we implied that DEPTOR may also play a protective role in asthma. In OVA mice, DEPTOR upregulation inhibited mucus hypersecretion and airway inflammation. Under normal conditions, the secretion of mucus prevents aspiration of foreign bodies and protects the airway [28]. However, in the pathological state, goblet cell proliferation and accompanying mucus hypersecretion are the main features of asthma [29], and MUC5AC is the major mucin expressed in asthma [30]. Our results showed that overexpression of DEPTOR suppressed the mucus occlusion and the expression of MUC5AC in OVA mice. Besides that, asthma is a chronic inflammatory disorder of the airways [31], and the effect of DEPTOR on inflammation was also evaluated. Overexpression of DEPTOR inhibited inflammatory cell infiltration and the release of inflammatory factors IL-4 and IL-5 in OVA mice. These findings implied that DEPTOR alleviates mucus hypersecretion and airway inflammation in OVA mice, thereby inhibiting the progression of asthma.

For deeper investigation, we found that DEPTOR inhibits ER stress and apoptosis in chondrocytes by directly regulating downstream protein activity, thereby alleviating the progression of osteoarthritis, and its function is independent of mTOR signaling [21]. ER stress plays a great part in disease development, including asthma. Studies have shown that ER stress interferes with protein synthesis and secretion and activates NF-κB to aggravate inflammation, which is involved in the development of diabetes, neurodegenerative diseases, pulmonary fibrosis, and asthma [32–34]. As we mentioned before, ER stress triggers a cascade of cellular signaling pathways, which is known as the UPR [35]. The three canonical branches of the UPR are mediated through three ER transmembrane proteins: inositol-requiring enzyme 1 (IRE1), activating transcription factor 6 (ATF6), and PKR-like eukaryotic initiation factor 2a kinase (PERK) [36]. Under basal conditions, the three UPR protein sensors are bound by GRP78, leaving them inactive [37]. Increased ER stress results in the recruitment of GRP78 away from these UPR sensors, which in turn activates to mitigate ER stress [38]. However, under persistent and severe ER stress, the UPR, in turn, aggravates cellular inflammation and induces apoptosis [10, 11]. For example, a representative ER stress-related apoptotic process is associated with the induction of the apoptotic transcription factor enhancer binding protein-homologous protein (CHOP), which is activated through the PERK pathway [39]. Moreover, all 3 canonical pathways of the UPR contribute to the induction of apoptotic responses when ER stress is excessive, persistent, or inadequately addressed [36]. Therefore,

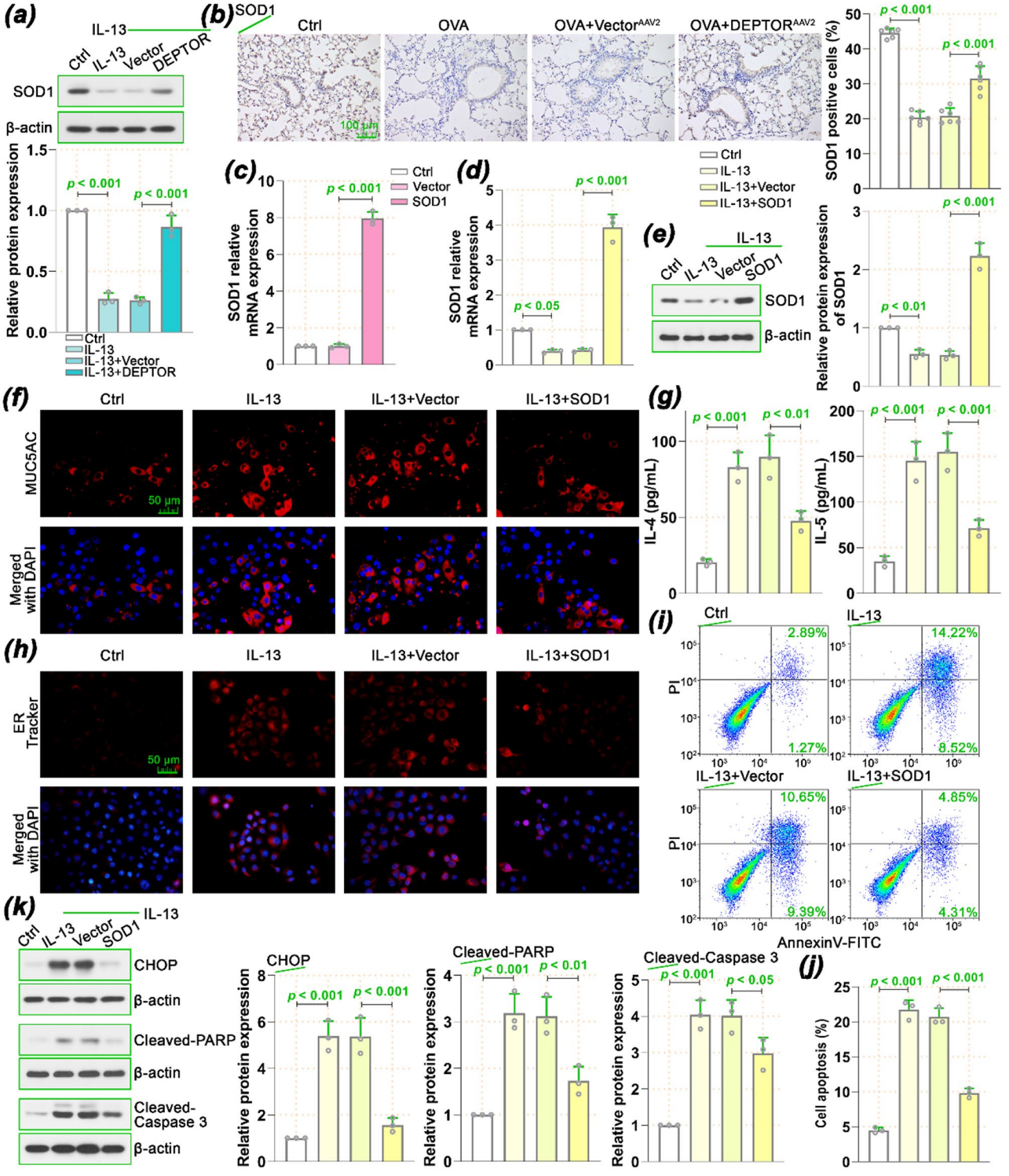

Fig. 7 Effect of SOD1 on asthma-induced malignant behaviors. (**a**) The protein expression of SOD1 in IL-13 treated 16HBE cells with DEPTOR overexpression. (**b**) The IHC staining images of SOD1 in lung tissues of OVA mice. (**c**) SOD1 was upregulated in 16HBE cells and the result was confirmed by qPCR. (**d-e**) The mRNA and protein expression of SOD1 in IL-13 treated 16HBE cells with SOD1 overexpression. (**f**) The IF staining images of MUC5AC in IL-13 treated 16HBE cells. (**g**) Levels of inflammatory cytokines IL-4 and IL-5 in IL-13 treated 16HBE cells. (**h**) IF technology traces ER in IL-13 treated 16HBE cells. (**i-j**) Cell apoptosis in IL-13 treated 16HBE cells was tested by flow cytometry. (**k**) Protein expression and quantification data of CHOP, cleaved-caspase-3, and cleaved-PARP in IL-13 treated 16HBE cells. Data were expressed as mean ± SD

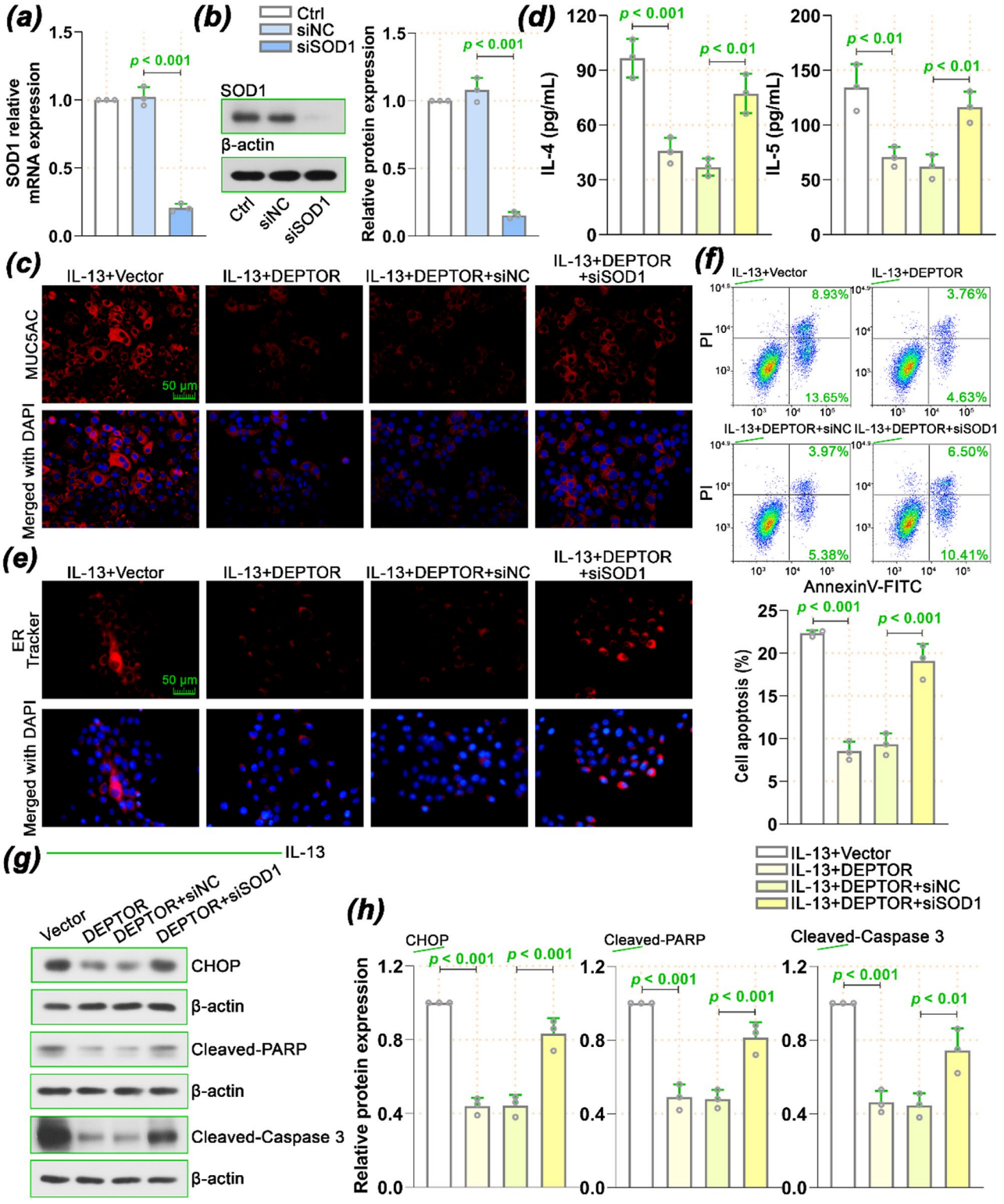

Fig. 8 SOD1 mediated the beneficial role of DEPTOR in asthma-induced malignant behaviors. (**a-b**) SOD1 was silenced in 16HBE cells and the result was confirmed by qPCR and western blot. (**c**) The IF staining images of MUC5AC in IL-13 treated 16HBE cells. (**d**) Levels of inflammatory cytokines IL-4 and IL-5 in IL-13 treated 16HBE cells. (**e**) IF technology traces ER in IL-13 treated 16HBE cells. (**f**) Cell apoptosis in IL-13 treated 16HBE cells was tested by flow cytometry. **(g-h)** Protein expression of CHOP, cleaved-caspase-3, and cleaved-PARP in IL-13 treated 16HBE cells. Data were expressed as mean ± SD

we explored whether DEPTOR plays an important role in asthma by regulating ER stress. Results showed that DEPTOR inhibits the expression of GPR78 and CHOP, and reduces the phosphorylation level of elf2 and nuclear ATF6 expression in OVA mice. In addition, DEPTOR inhibited cell apoptosis and decreased the expression of cleaved-PARP and cleaved-caspase 3 in OVA mice. Similar results were obtained in IL-13 treated 16HBE cells. Accordingly, these results confirmed that DEPTOR suppressed ER stress, and UPR activation and followed cell apoptosis in asthma.

To explore the factors that may be regulated by DEPTOR, we performed proteomics in IL-13 treated 16HBE cells. From the results, it can be seen that overexpression of DEPTOR significantly affected the protein expression of several genes. Among these differentially expressed proteins, SOD1 caught our attention (top 10 upregulated proteins). SOD1 is an important antioxidant enzyme that is well known for its ROS-scavenging activity. In IL-13 treated 16HBE cells, upregulation of DEPTOR enhanced the protein expression of SOD1 ($Log_2FC=3.48$, $p<0.05$). From reported studies, we found that loss of SOD1 in mammalian cells leads to cell death due to the accumulation of oxidative stress [40]. Upregulation of SOD1 has been shown to reduce ROS production, thereby inhibiting oxidative stress and attenuating ER stress-induced apoptosis in vascular endothelial cells [26]. Besides that, SOD1 overexpression in the lung prevents PM2.5-induced cell death and alveolar-capillary barrier dysfunction in mice [41]. In asthma, targeted inhibition of SOD1 in the lung tissue of asthmatic mice aggravated inflammatory responses and asthma symptoms [42]. Thus, we suggested that SOD1 may act as a downstream factor of DEPTOR that mediates the protective effect of DEPTOR in asthma.

After that, we confirmed the expression of SOD1 in DEPTOR-upregulated 16HBE cells and OVA mice. Results displayed that upregulation of DEPTOR promoted the expression of SOD1 both in IL-13 induced 16HBE cells and OVA mice. Furthermore, the upregulation of SOD1 also has a beneficial effect on asthma progression. Rescue experiments showed that SOD1 knockdown attenuates the beneficial effects of DEPTOR on mucus hypersecretion, inflammation, ER stress, and cell apoptosis in IL-13 induced 16HBE cells. This finding is consistent with previous reports of a role for SOD1 in asthma, where inhibition of SOD1 exacerbates the progression of asthma [42]. Our results further exhibited that the beneficial effect of SOD1 in asthma may be related to its inhibitory effect on ER stress.

Besides that, our current study also has some limitations and places for further investigation. First, DEPTOR is an endogenous mTOR inhibitor, and mTOR plays an important role in asthma [43]. Also, a reported study has confirmed that mTOR can inhibit SOD1 activity [44]. Based on this, we confirmed the effect of DEPTOR on the mTOR pathway in OVA mice. As shown in Fig. S1, OVA treatment promoted the phosphorylation level of mTOR, and the upregulation of DEPTOR significantly inhibited the expression of p-mTOR ($p<0.05$). Therefore, we suspected that DEPTOR may either directly regulate the expression of SOD1 or upregulate SOD1 by inhibiting the activity of the mTOR pathway. Second, the current studies on DEPTOR were mainly focused on cancer, but little is known about its role in asthma. Third, this study focused on the regulation of SOD1 protein levels by DEPTOR. Therefore, in subsequent studies, we may explore the upstream regulators of DEPTOR and SOD1, to further investigate the specific mechanism of its downregulation in asthma.

In conclusion, our results suggested that DEPTOR alleviates the progression of asthma through the inhibition effect on ER stress, and SOD1 participated in this progression.

Supplementary Information

The online version contains supplementary material available at https://doi.org/10.1186/s13062-024-00557-z.

Supplementary Material 1

Author contributions

Hao Wang contributed to the study conception and design, performed experiments, analyzed data, and drafted the manuscript. Lei Zhang performed experiments and analyzed data. Yunxiao Shang revised the manuscript. All authors agree to submit this manuscript.

Funding

This research received no funding.

Data availability

The data generated and analyzed during the current study are available from the corresponding author upon reasonable request.

Declarations

Ethical approval

All animal experiments were approved by the Institutional Animal Care and Use Committee of Shengjing Hospital of China Medical University (code: 2023PS737K).

Competing interests

The authors declare no competing interests.

Received: 4 July 2024 / Accepted: 1 November 2024
Published online: 12 November 2024

References

1. Ntontsi P, Photiades A, Zervas E, Xanthou G, Samitas K. Genetics and epigenetics in Asthma. Int J Mol Sci. 2021;22(5).
2. Porsbjerg C, Melén E, Lehtimäki L, Shaw D, Asthma. Lancet. 2023;401(10379):858–73.
3. Papi A, Brightling C, Pedersen SE, Reddel HK. Asthma Lancet. 2018;391(10122):783–800.

4. Volta CA, Dalla Corte F, Ragazzi R, Marangoni E, Fogagnolo A, Scaramuzzo G, et al. Expiratory flow limitation in intensive care: prevalence and risk factors. Crit Care. 2019;23(1):395.
5. Aaron SD, Boulet LP, Reddel HK, Gershon AS. Underdiagnosis and overdiagnosis of Asthma. Am J Respir Crit Care Med. 2018;198(8):1012–20.
6. Reddel HK, Bacharier LB, Bateman ED, Brightling CE, Brusselle GG, Buhl R, et al. Global Initiative for Asthma Strategy 2021: executive Summary and Rationale for Key Changes. Am J Respir Crit Care Med. 2022;205(1):17–35.
7. Ortega H, Hahn B, Tran JN, Bell C, Shams SA, Llanos JP. Disease burden in patients with asthma before initiating biologics: a retrospective cohort database study. Allergy Asthma Proc. 2019;40(3):146–53.
8. Oakes SA, Papa FR. The role of endoplasmic reticulum stress in human pathology. Annu Rev Pathol. 2015;10:173–94.
9. Marciniak SJ, Chambers JE, Ron D. Pharmacological targeting of endoplasmic reticulum stress in disease. Nat Rev Drug Discov. 2022;21(2):115–40.
10. Wang M, Kaufman RJ. Protein misfolding in the endoplasmic reticulum as a conduit to human disease. Nature. 2016;529(7586):326–35.
11. Yan M, Shu S, Guo C, Tang C, Dong Z. Endoplasmic reticulum stress in ischemic and nephrotoxic acute kidney injury. Ann Med. 2018;50(5):381–90.
12. Kim SR, Kim DI, Kang MR, Lee KS, Park SY, Jeong JS, et al. Endoplasmic reticulum stress influences bronchial asthma pathogenesis by modulating nuclear factor κB activation. J Allergy Clin Immunol. 2013;132(6):1397–408.
13. Pathinayake PS, Hsu AC, Waters DW, Hansbro PM, Wood LG, Wark PAB. Understanding the unfolded protein response in the pathogenesis of Asthma. Front Immunol. 2018;9:175.
14. Bhakta NR, Christenson SA, Nerella S, Solberg OD, Nguyen CP, Choy DF, et al. IFN-stimulated gene expression, type 2 inflammation, and endoplasmic reticulum stress in Asthma. Am J Respir Crit Care Med. 2018;197(3):313–24.
15. Bradley KL, Stokes CA, Marciniak SJ, Parker LC, Condliffe AM. Role of unfolded proteins in lung disease. Thorax. 2021;76(1):92–9.
16. Caron A, Briscoe DM, Richard D, Laplante M. DEPTOR at the Nexus of Cancer, Metabolism, and immunity. Physiol Rev. 2018;98(3):1765–803.
17. Doan H, Parsons A, Devkumar S, Selvarajah J, Miralles F, Carroll VA. HIF-mediated suppression of DEPTOR confers resistance to mTOR kinase inhibition in Renal Cancer. iScience. 2019;21:509–20.
18. Ouyang Z, Kang D, Li K, Liang G, Liu Z, Mai Q, et al. DEPTOR exacerbates bone-fat imbalance in osteoporosis by transcriptionally modulating BMSC differentiation. Volume 151. Biomedicine & pharmacotherapy = Biomedecine & pharmacotherapie; 2022. p. 113164.
19. Catena V, Fanciulli M. Deptor: not only a mTOR inhibitor. J Experimental Clin cancer Research: CR. 2017;36(1):12.
20. Chen H, Shen F, Sherban A, Nocon A, Li Y, Wang H, et al. DEP domain-containing mTOR-interacting protein suppresses lipogenesis and ameliorates hepatic steatosis and acute-on-chronic liver injury in alcoholic liver disease. Hepatology. 2018;68(2):496–514.
21. Li K, Yang P, Zhang Y, Zhang Y, Cao H, Liu P, et al. DEPTOR prevents Osteoarthritis Development Via Interplay with TRC8 to reduce endoplasmic reticulum stress in Chondrocytes. J bone Mineral Research: Official J Am Soc Bone Mineral Res. 2021;36(2):400–11.
22. Zhan JB, Zheng J, Zeng LY, Fu Z, Huang QJ, Wei X, et al. Downregulation of mir-96-5p inhibits mTOR/NF-κb signaling pathway via DEPTOR in allergic Rhinitis. Int Arch Allergy Immunol. 2021;182(3):210–9.
23. Zhu T, Zhang W, Wang DX, Huang NW, Bo H, Deng W, et al. Rosuvastatin attenuates mucus secretion in a murine model of chronic asthma by inhibiting the gamma-aminobutyric acid type A receptor. Chin Med J (Engl). 2012;125(8):1457–64.
24. Xu X, Kwon OK, Shin IS, Mali JR, Harmalkar DS, Lim Y, et al. Novel benzofuran derivative DK-1014 attenuates lung inflammation via blocking of MAPK/AP-1 and AKT/mTOR signaling in vitro and in vivo. Sci Rep. 2019;9(1):862.
25. Wiseman RL, Mesgarzadeh JS, Hendershot LM. Reshaping endoplasmic reticulum quality control through the unfolded protein response. Mol Cell. 2022;82(8):1477–91.
26. Ei ZZ, Hutamekalin P, Prommeenate P, Singh A, Benjakul S, Visuttijai K, et al. Chitooligosaccharide prevents vascular endothelial cell apoptosis by attenuation of endoplasmic reticulum stress via suppression of oxidative stress through Nrf2-SOD1 up-regulation. Pharm Biol. 2022;60(1):2155–66.
27. Barcik W, Boutin RCT, Sokolowska M, Finlay BB. The role of lung and gut microbiota in the Pathology of Asthma. Immunity. 2020;52(2):241–55.
28. Lu Y, Xing QQ, Xu JY, Ding D, Zhao X. Astragalus polysaccharide modulates ER stress response in an OVA-LPS induced murine model of severe asthma. Int J Biol Macromol. 2016;93(Pt A):995–1006.
29. Rogers DF. The airway goblet cell. Int J Biochem Cell Biol. 2003;35(1):1–6.
30. Livraghi-Butrico A, Grubb BR, Wilkinson KJ, Volmer AS, Burns KA, Evans CM, et al. Contribution of mucus concentration and secreted mucins Muc5ac and Muc5b to the pathogenesis of muco-obstructive lung disease. Mucosal Immunol. 2017;10(2):395–407.
31. Ray A, Kolls JK. Neutrophilic Inflammation in Asthma and Association with Disease Severity. Trends Immunol. 2017;38(12):942–54.
32. Villalobos-Labra R, Subiabre M, Toledo F, Pardo F, Sobrevia L. Endoplasmic reticulum stress and development of insulin resistance in adipose, skeletal, liver, and foetoplacental tissue in diabesity. Mol Aspects Med. 2019;66:49–61.
33. Martínez G, Khatiwada S, Costa-Mattioli M, Hetz C. ER Proteostasis Control of Neuronal Physiology and synaptic function. Trends Neurosci. 2018;41(9):610–24.
34. Wang Y, Zhu J, Zhang L, Zhang Z, He L, Mou Y, et al. Role of C/EBP homologous protein and endoplasmic reticulum stress in asthma exacerbation by regulating the IL-4/signal transducer and activator of transcription 6/transcription factor EC/IL-4 receptor α positive feedback loop in M2 macrophages. J Allergy Clin Immunol. 2017;140(6):1550–e618.
35. Dastghaib S, Kumar PS, Aftabi S, Damera G, Dalvand A, Sepanjnia A, et al. Mechanisms targeting the unfolded protein response in Asthma. Am J Respir Cell Mol Biol. 2021;64(1):29–38.
36. Kim SR, Lee YC. Endoplasmic reticulum stress and the related signaling networks in severe asthma. Allergy Asthma Immunol Res. 2015;7(2):106–17.
37. Bertolotti A, Zhang Y, Hendershot LM, Harding HP, Ron D. Dynamic interaction of BiP and ER stress transducers in the unfolded-protein response. Nat Cell Biol. 2000;2(6):326–32.
38. Hetz C. The unfolded protein response: controlling cell fate decisions under ER stress and beyond. Nat Rev Mol Cell Biol. 2012;13(2):89–102.
39. Osorio F, Lambrecht B, Janssens S. The UPR and lung disease. Semin Immunopathol. 2013;35(3):293–306.
40. Banks CJ, Andersen JL. Mechanisms of SOD1 regulation by post-translational modifications. Redox Biol. 2019;26:101270.
41. Soberanes S, Urich D, Baker CM, Burgess Z, Chiarella SE, Bell EL, et al. Mitochondrial complex III-generated oxidants activate ASK1 and JNK to induce alveolar epithelial cell death following exposure to particulate matter air pollution. J Biol Chem. 2009;284(4):2176–86.
42. Wang L, Xu J, Liu H, Li J, Hao H. PM2.5 inhibits SOD1 expression by up-regulating microRNA-206 and promotes ROS accumulation and disease progression in asthmatic mice. Int Immunopharmacol. 2019;76:105871.
43. Zhang Y, Jing Y, Qiao J, Luan B, Wang X, Wang L, et al. Activation of the mTOR signaling pathway is required for asthma onset. Sci Rep. 2017;7(1):4532.
44. Tsang CK, Chen M, Cheng X, Qi Y, Chen Y, Das I, et al. SOD1 phosphorylation by mTORC1 couples nutrient sensing and Redox Regulation. Mol Cell. 2018;70(3):502–e158.

Publisher's note